


RESEARCH ARTICLE

Glycolytic lactate production supports status epilepticus in experimental animals

Daria Skwarzynska¹, Huayu Sun², Izabela Kasprzak², Supriya Sharma², John Williamson² & Jaideep Kapur^{2,3} 

¹Neuroscience Graduate Program, University of Virginia, Charlottesville, Virginia, 22908, USA

²Department of Neurology, University of Virginia, Charlottesville, Virginia, 22908, USA

³UVA Brain Institute, University of Virginia, Charlottesville, Virginia, 22908, USA

Correspondence

Jaideep Kapur, UVA Brain Institute, University of Virginia, Health Sciences Center, PO Box: 801330, Charlottesville, VA 22908, USA. Fax: (434) 924-8666; E-mail: jk8t@virginia.edu

Received: 20 June 2023; Revised: 27 July 2023; Accepted: 9 August 2023

Annals of Clinical and Translational Neurology 2023; 10(10): 1873–1884

doi: 10.1002/acn3.51881

Abstract

Objective: Status epilepticus (SE) requires rapid intervention to prevent cerebral injury and mortality. The ketogenic diet, which bypasses glycolysis, is a promising remedy for patients with refractory SE. We tested the role of glycolytic lactate production in sustaining SE. **Methods:** Extracellular lactate and glucose concentration during a seizure and SE in vivo was measured using lactate and glucose biosensors. A lactate dehydrogenase inhibitor, oxamate, blocked pyruvate to lactate conversion during SE. Video-EEG recordings evaluated seizure duration, severity, and immunohistochemistry was used to determine neuronal loss. Genetically encoded calcium indicator GCaMP7 was used to study the effect of oxamate on CA1 pyramidal neurons in vitro. Spontaneous excitatory postsynaptic currents (sEPSCs) were recorded from CA1 neurons to study oxamate's impact on neurotransmission. **Results:** The extracellular glucose concentration dropped rapidly during seizures, and lactate accumulated in the extracellular space. Inhibition of pyruvate to lactate conversion with oxamate terminated SE in mice. There was less neuronal loss in treated compared to control mice. Oxamate perfusion decreased tonic and phasic neuronal activity of GCaMP7-expressing CA1 pyramidal neurons in vitro. Oxamate application reduced the frequency, but not amplitude of sEPSCs recorded from CA1 neurons, suggesting an effect on the presynaptic glutamatergic neurotransmission. **Interpretation:** A single seizure and SE stimulate lactate production. Diminishing pyruvate to lactate conversion with oxamate terminated SE and reduced associated neuronal death. Oxamate reduced neuronal excitability and excitatory neurotransmission at the presynaptic terminal. Glycolytic lactate production sustains SE and is an attractive therapeutic target.

Introduction

Status epilepticus (SE) is a neurological emergency requiring intervention to prevent cerebral injury and mortality. When first- and second-line anti-seizure medications fail to terminate seizures, SE is considered refractory (RSE). The current treatment strategy for RSE uses intravenous anesthetic agents for ≥ 24 h to suppress seizures. SE is considered super refractory (SRSE) if seizures continue after anesthetic treatment. The overall mortality associated with both RSE and SRSE ranges from 23 to 57%.¹ The ketogenic diet (KD), a high-fat, low-carbohydrate diet,

has emerged as a treatment option in adult² and pediatric patients with epilepsy.^{3,4} Recently, KD was used to manage RSE and SRSE.^{1,5,6}

Despite the broad application of KD in clinical settings, surprisingly, little is known about its underlying mechanism of action. The therapeutic effect of KD can result from the production of ketone bodies.^{7,8} Ketone bodies provide an alternative fuel to glucose for energy production by supplying acetyl-CoA to the tricarboxylic acid cycle (TCA). The concept that KD, via ketone bodies, bypasses glycolysis gave rise to the possibility that inhibiting glycolysis can prevent seizures. The glucose analog,

2-deoxyglucose (2-DG), initially used to map brain regions involved in seizures,⁹ emerged as a glycolysis inhibitor and an anti-seizure medication.^{10,11} 2-DG converts to phosphorylated 2-DG (2-DG-P) in the first reaction of glycolysis, which does not undergo further metabolism, thereby inhibiting glycolysis. Cell membrane permeability to 2-DG-P is low.¹² Thus, trapped 2-DG-P accumulates inside the cell.¹³ 2-DG inhibits seizure-like events in vitro^{14,15} and seizures in vivo,¹⁵ and SE in neonatal rats.¹⁶ Additionally, 2-DG is a well-studied anticancer agent in the preclinical models.¹⁷ Despite the initially encouraging results, preliminary data from clinical trials are inconclusive. The recommended, safe dose of 2-DG in the phase I dose-escalation trial in prostatic cancer did not produce the intended results.¹⁷ Additionally, higher doses of 2-DG were associated with hyperglycemia and altered cardio-respiratory function in animal models.¹⁸ However, more recent studies at clinically effective doses of 2-DG do not exert such adverse effects.¹⁹

Cells produce energy by generating lactate when oxidative phosphorylation is insufficient.²⁰ Glycolysis produces 2 ATP molecules by shunting pyruvate away from mitochondria and converting it to lactate by the enzyme lactate dehydrogenase (LDH) when there is tissue hypoxia or when oxidative phosphorylation is inadequate to sustain energy demands, as observed in rapidly contracting muscle. Thus, pyruvate-to-lactate conversion allows for the more rapid production of ATP.²¹

LDH has recently attracted attention as a potential regulator of energy metabolism in several brain conditions, including cancer²² and epilepsy.^{23–27} LDH-catalyzed reduction of pyruvate to lactate regenerates NAD⁺ from NADH. NAD⁺ is an obligatory substrate for one of the steps in the glycolytic pathway, the conversion of glyceraldehyde-3-phosphate to 1,3-diphosphoglycerate. Therefore, NAD⁺ facilitates glycolysis. Targeting LDH activity is an alternative approach to 2-DG to inhibit anaerobic glycolysis while oxidative phosphorylation can continue. Two LDH inhibitors, oxamate, and NHI-1 were shown to suppress seizures²⁴ and spontaneous paroxysmal discharges in chronic seizure models in vivo.²³

Nonetheless, several questions remain unanswered. First, it is unclear whether blocking lactate production with the LDH inhibitor oxamate effectively terminates SE in adult rodents. Secondly, SE termination with a glycolysis inhibitor could worsen neuronal damage. Finally, the cellular mechanism underlying the anti-seizure effect of lactate inhibition is unknown. We investigated the extracellular glucose and lactate concentration during a single seizure and SE in vivo. Then, we tested whether inhibition of pyruvate to lactate conversion with oxamate could terminate SE and reduce SE-associated neuronal loss.

Finally, we studied oxamate's action on the neuronal network, individual neurons, and synaptic transmission.

Methods

Animals

We used 4- to 8-week-old c57bl/6 mice (Charles River, North Carolina) of both sexes. University of Virginia Care and Use Committee approved all experimental protocols. We housed them five per cage, gave them ad libitum access to food and water, and maintained them on a 12 h light / 12 h dark cycle.

Lactate and glucose concentration measurement during a single seizure and status epilepticus

Lactate or glucose concentration during a single seizure and SE was measured using a lactate oxidase-based and a glucose oxidase-based biosensor probe (Pinnacle Technologies, KS, USA) with simultaneous video-EEG monitoring.²⁸ We designed the recording assembly composed of an intracranial guide cannula (biosensor insertion) with an attached hippocampal recording electrode. The assembly consisted of a cortical electrode ipsilateral, a reference electrode, and a bipolar-insulated stainless-steel stimulating electrode contralateral to the probe. We stereotactically implanted 7- to 8-week-old C57Bl/6 mice with the cannula and a hippocampal recording electrode in the left CA1 (−3 mm anteroposterior, −3 mm mediolateral, 3 mm dorsoventral), stimulating electrode in the right CA1 (−3 mm anteroposterior, 3 mm mediolateral, 3 mm dorsoventral), unilateral cortical electrode, and a cerebellar reference electrode. A week after the surgery, we connected the animals to a video-EEG monitoring system (Lab chart software, ADInstruments) via a flexible cable connected to the amplifier. Biosensors were calibrated according to the manufacturer's manual before insertion into the brain and recalibrated after the experiment. Briefly, analyte solutions were made fresh on the day of the calibration. Pre- and post-calibration was performed for each biosensor probe, that is, the rising concentration of the analyte of interest (D-glucose for a glucose biosensor probe and L-lactate for a lactate biosensor probe), injection of the interference solution (ascorbic acid) followed by a final injection of the analyte. Animals were subjected to seizure and SE induction protocols, as described previously.²⁸ Animals were monitored by continuous video-EEG with simultaneous lactate or glucose concentration measurements until the end of the seizures and SE.

Electrode implantation, induction of status epilepticus, and oxamate treatment

Mice were injected intraperitoneally with saline or sodium oxamate (1 g/kg) (Abcam, ab145643) 15 min after self-sustaining SE developed. The end of SE was defined as a decline in spike-wave discharge frequency below 1 Hz. We scored behavioral seizures using a modified Racine scale²⁹ as previously described.^{28,30,31}

Immunohistochemistry and imaging

Animals were perfused transcardially with 4% paraformaldehyde (PFA) in 0.1 M phosphate buffer (PB). The brains were harvested and postfixed in 4% PFA solution overnight and cryoprotected in 30% sucrose for 48 h. Immunohistochemistry was performed as previously described.^{32,33} The brains were sliced into thin (40 μ m) coronal sections on a cryostat (Precisionary, CF-6100) and processed for immunohistochemistry. Anti-NeuN antibody (1:500, MAB377, Millipore) and DAPI were used to stain the free-floating brain sections. Imaging was performed using a confocal microscope (Nikon Eclipse Ti-U at 10 \times magnification, 0.45 NA). Excitation lasers were 488 nm for green and 405 nm for blue. Images were tiled as stacks with optical section separation (Z interval) of 5 μ m and stitched using NIS Elements software. Imaris 9.3.0 (Bitplane) was used for visualizing, and Adobe Photoshop CC was used for cropping the original image and display.

Evaluation of CA1 neuronal loss

We studied neuronal loss using previously described methods.³⁴ NeuN immunoreactivity in the CA1 layer was counted semi-automatically. We computed the maximum intensity projection image (MIP) for the green (NeuN) channel and converted them into grayscale for counting. To avoid bias, we maintained the coronal slices' coordinates for saline- and oxamate-treated animals and verified the location from the Allen atlas.

In vivo viral transfection

We used a mix of pENN.AAV.CamKII 0.4.Cre.SV40 and pGP-AAV-syn-FLEX-jGCaMP7s-WPRE (Addgene, viral titer 1×10^{13} vg/mL) viruses to study calcium dynamics in vitro. The virus was injected as described previously.^{28,31} Briefly, p30-40 C57Bl/6 mice were stereotactically injected with a mix of viruses in the ratio 1:1 bilaterally in the ventral and dorsal CA1 (anteroposterior, -2.54 ; mediolateral, ± 2.00 ; dorsoventral, -1.20 , and AP, -3.40 ; ML, ± 3.35 ; DV, -2.25). A Hamilton syringe (Hamilton 7000 Glass, 5 μ L, 0.3302 mm, Reno, NV) was loaded with a virus

solution and mounted in the peristaltic pump holder (Harvard Apparatus, Holliston, MA; P-1500). The virus mixture was infused at 0.1 μ L/min constant flow rate and 0.100 μ L per location. Mice were euthanized, and tissue was processed 10–14 days after the surgery for GCaMP7 imaging.

Acute hippocampal slice preparation

We sliced brains into 300 μ m coronal sections containing the hippocampus with a vibratome (VT1200S; Leica, Wetzlar, Germany) in an ice-cold, oxygenated slicing buffer comprising (mM): 65.5 NaCl, 2 KCl, 5 MgSO₄, 1.1 KH₂PO₄, 1 CaCl₂, 10 dextrose, and 113 sucrose (300 mOsm). The slices were then placed in an interface chamber containing oxygenated artificial cerebrospinal fluid (aCSF) containing: (in mM) 124 NaCl, 4 KCl, 1 MgCl₂, 25.7 NaHCO₃, 1.1 KH₂PO₄, 10 dextrose, and 2.5 CaCl₂ (300 mOsm) at room temperature (25°C) and allowed to equilibrate for 30 min.

In vitro imaging of genetically encoded calcium indicator

GCaMP7 signals were imaged on an inverted epifluorescence microscope (Nikon Eclipse Ti, Japan) with a GFP filter set (Nikon, Intensilight C-HGFIE, Japan) and NIS Elements Advanced Research (AR) Software (5.21.03). The wide-field imaging system consisted of a microscope (Nikon Eclipse Ti, Japan) equipped with a motorized stage system (OptiScanTMIII, Prior Scientific Instruments Ltd, Cambridge, UK), Z-focus controller (NIKRFK, Prior Scientific Instruments Ltd, Cambridge, UK), an automated light shutter (Prior Scientific, Ltd, OptiScan III), and a high quantum efficiency camera (ORCA-Fusion BT, Hamamatsu, c15440-20UP, Japan). Light from a LED source was filtered for excitation at 488 and 525 nm for emission collection. Images were acquired at 0.2 Hz. Changes in calcium fluorescence were measured in ROIs comprising the GCaMP7-positive CA1 pyramidal cell bodies. Potassium concentration in the aCSF was increased from 2 mM (baseline aCSF) to 5 mM (high K⁺ aCSF) to excite the neuronal network. Slices were perfused with high K⁺ aCSF containing 3 mM sodium oxamate (Sigma) to study the effect of oxamate on the excited population of CA1 neurons. A wash-out step with high K⁺ aCSF was performed for each slice to ensure slice health and function.

Image analysis

Time-lapse movies were analyzed as previously described.²⁸ Time-lapse movies were uploaded into ImageJ, and a region of interest (ROI) was drawn. The

multi-measure functionality was used for pixel measurements for all images. All measured fluorescent values were normalized to baseline and expressed as a % change in fluorescence ($\% \Delta F/F$).

Electrophysiology

CA1 neurons were visually identified on an upright microscope (Nikon Eclipse E600FN) with a 40X water-immersion objective (Nikon, NA = 0.8) and a camera (Nikon DS2 Qi). Spontaneous excitatory postsynaptic currents were recorded from CA1 principal neurons using standard voltage-clamp patch-clamp electrophysiology techniques at 30°C.³⁵ D-2-amino-5-phosphonopentanoic acid (APV, 50 μ M) (Tocris) was added to prevent NMDA receptor-mediated plasticity, and GABA_A receptor antagonist, picrotoxin (Sigma-Aldrich), was added (100 μ M) to block inhibitory transmission. Currents were filtered at 2 kHz, digitized using a Digidata 1322 digitizer (Molecular Devices, Sunnyvale, CA, USA), and acquired using Clampex 10.2 software (Molecular Devices).

Statistical analysis

T-test, Wilcoxon matched-pairs signed-rank test, Kolmogorov–Smirnov test, Fisher test, Kaplan–Meier survival comparison, Mantel–Cox long-rank test, two-tailed Mann–Whitney test, and one-way ANOVA with post hoc Bonferroni correction were performed using GraphPad Prism software. *p* value <0.05 was considered significant.

Results

Seizures rapidly stimulate anaerobic glycolysis

Glucose is converted to pyruvate during glycolysis. Pyruvate is converted to acetyl-coenzyme A (acetyl-CoA) by pyruvate dehydrogenase (PDH) and further oxidized in the tricarboxylic acid cycle (TCA). Alternatively, during anaerobic glycolysis, pyruvate is reduced to lactate by LDH and NADH to NAD⁺ (Fig. 1A). Then, a monocarboxylate transporter (MCT) transports lactate into the extracellular space. Thus, extracellular glucose and lactate concentration serve as a proxy to estimate changes in the rate of glycolysis.

We studied real-time changes in the extracellular concentration of glucose and lactate during a single, non-convulsive seizure and SE in vivo (Fig. 1A,B). The baseline extracellular glucose and lactate concentration were stable over time (lactate: *n* = 5; 387 μ M; glucose: *n* = 4; 783 μ M). An electrical stimulation protocol²⁸ induced a single seizure. Even a short seizure rapidly accelerated

glucose metabolism, as demonstrated by a quick drop in extracellular glucose concentration and increased lactate concentration (Fig. 1C,D). Moreover, we detected an altered concentration of both metabolites in the extracellular space for minutes (<15 min), which suggests that even a single seizure alters brain glucose metabolism for minutes, even after the restoration of normal EEG.

After allowing glucose and lactate levels to return to baseline, we investigated the real-time changes in glucose and lactate concentration in the hippocampus during SE. First, we induced SE by CHS in mice^{28,30} implanted with either lactate or glucose probes. We detected a rapid increase in the extracellular lactate concentration during electrical stimulation and the self-sustaining phase of SE (Fig. 1E). The seizure activity during SE consists of rhythmic high-amplitude low-frequency epileptiform discharges interspersed with short bouts of high-frequency events. We found that high-frequency discharges were associated with a larger lactate buildup in the extracellular space than the persistent high-amplitude slow epileptiform discharges (Fig. 1F). To further describe the extracellular lactate level during SE in the population studied (*n* = 4), the period from the beginning of the self-sustaining phase of SE to the termination of SE was divided into quartiles. Extracellular lactate levels were highest during the first quartile of SE (Fig. 1E,G), associated with the highest power in each EEG frequency band and more frequent fast discharges.³⁰ The extracellular lactate level decreased as SE became less severe over time.³⁰ The waning phase of SE was associated with the lower lactate level (Fig. 1E,G), but the elevated lactate level persisted even after SE ended.

We detected a transient drop in the extracellular glucose concentration and rapid recovery during the 60-minute stimulation (Fig. 1H). The post-stimulation phase of SE was associated with high extracellular glucose fluctuations (Fig. 1H). Interestingly, we observed a delay in the extracellular glucose response to the fast discharges (Fig. 1I). Glucose level fluctuated during the first quartile of SE, a less variable glucose concentration declined during the following three quartiles. Brain glucose was ~50% of the baseline at the end of SE. These studies indicate that glucose metabolism fuels SE, especially during the first two quartiles of SE (Fig. 1). Thus, we tested whether inhibition of pyruvate to lactate conversion effectively terminates SE.

Oxamate terminated SE

We induced SE by the CHS model.^{28,30,31} Mice were then randomly assigned to the treatment or control group. Mice received an IP injection of either oxamate (1 g/kg) or saline 15 min after the development of self-sustaining SE

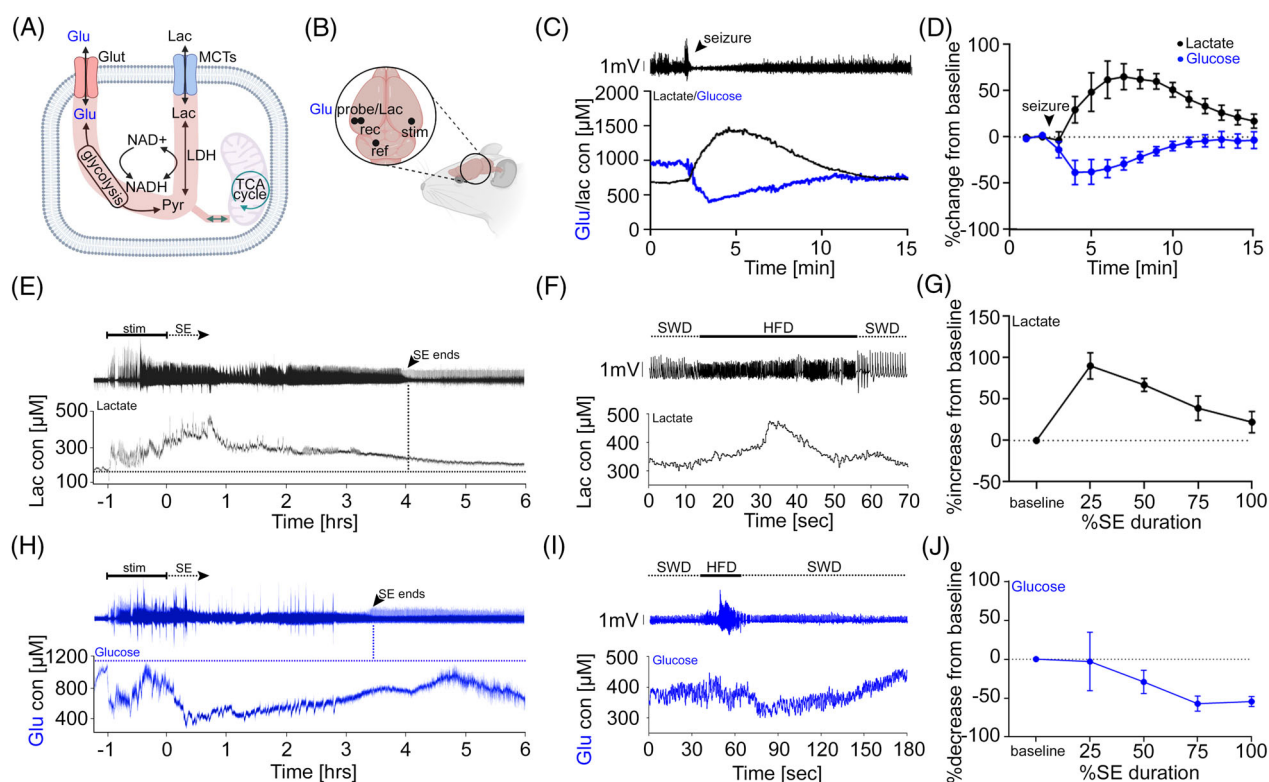


Figure 1. Seizures stimulate anaerobic glycolysis. (A) A simplified cartoon of the glycolysis pathway. (B) Diagram of study design. A custom-built recording assembly was inserted into the ventral CA1 hippocampus. Brief and non-convulsive seizures were induced by an electrical stimulus. Status epilepticus was induced by continuous hippocampal stimulation. Extracellular glucose/lactate concentration and EEGs were recorded simultaneously. (C) Seizures stimulate anaerobic glycolysis. Fast changes in the extracellular glucose and lactate concentration in the hippocampus during a seizure. *Top*: a section of EEG recorded from the electrode ipsilateral to the lactate biosensor. *Bottom*: representative traces of extracellular glucose (blue) and lactate (black) concentration. Seizures stimulate rapid glucose uptake and lactate production. (D) Seizures rapidly accelerate anaerobic glycolysis. A brief seizure episode quickly stimulates extracellular glucose consumption ($n = 4$) and lactate release to the extracellular space ($n = 5$). (E) Lactate fluctuations during SE. *Top*: a section of EEG recorded from the electrode ipsilateral to the lactate biosensor. *Bottom*: extracellular lactate level. Note the increase in lactate concentration during stimulation (stim) and the self-sustaining phase of SE and the drop in extracellular lactate level when SE ends. (F) Fast discharges stimulate lactate production. *Top*: a section of EEG from *E* representing rhythmic high-amplitude slow discharges and high- and low-amplitude fast discharges *bottom*: corresponding lactate level. Note immediate lactate increase in the extracellular space during fast discharges. (G) Extracellular lactate level during SE plotted against % of the SE duration. Note the drastic increase in extracellular lactate concentration during the 1 quartile of SE and decrease as SE continues. Extracellular lactate concentration remains elevated when SE terminates. (H) Glucose fluctuations during SE. *Top*: a section of EEG recorded from the electrode ipsilateral to the lactate biosensor. *Bottom*: extracellular glucose level. Note the initial decrease in glucose concentration during stimulation (stim) and the sudden elevation of glucose in the extracellular space during the later phase of stimulation. During the self-sustaining phase of SE, glucose fluctuates and marginally recovers when SE ends. (I) High-frequency discharges stimulate glucose uptake. *Top*: a section of EEG from *H*, *bottom*: corresponding glucose level. Note the delay in glucose response. (J) Extracellular glucose level during SE plotted against % of the SE duration. Note the variable response in the extracellular glucose level during the 1 quartile of SE and decrease as SE continues.

(Fig. 2A). We found that SE was significantly shorter in oxamate-treated mice than saline-injected mice ($n = 5$ oxamate, $n = 8$ control; $p < 0.05$, Kaplan–Meier survival comparison followed by Mantel–Cox long-rank test) (Fig. 2B). Additionally, we detected fewer high-frequency discharges following oxamate treatment, which indicates that oxamate's action quickly hindered the highly energy-consuming events (Fig. 2D,E) ($n = 5$ in each group, $p < 0.005$, Kolmogorov–Smirnov test). Moreover,

oxamate-treated mice returned to normal behavior faster than control mice ($n = 5$ each; $p < 0.001$, two-tailed Mann–Whitney test) (Fig. 2F).

The postictal state characterizes a rich set of neurological deficits in humans, such as unresponsiveness, headaches, and psychosis, which strongly affect patients' quality of life.³⁶ Additionally, intermittent epileptiform discharges (postictal spikes) occur following SE in experimental animals³⁰ and patients. Moreover, post-SE and

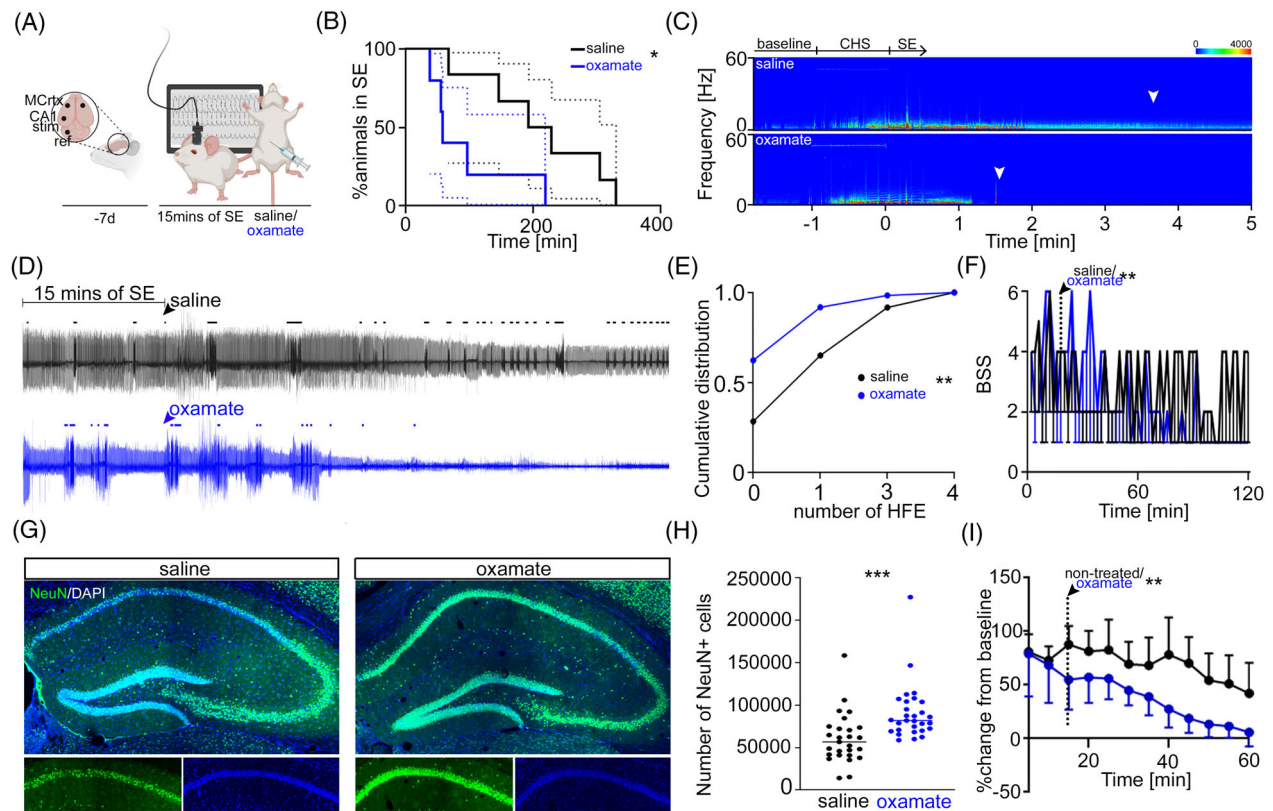


Figure 2. Oxamate terminates status epilepticus. (A) Diagram of study design. A stimulating electrode was inserted in the ventral CA1 hippocampus and recording electrodes in the cortex bilaterally. Status epilepticus (SE) was induced a week later (methods section). Mice were video and EEG-monitored. (B) SE duration in saline- and oxamate-treated mice. SE in oxamate-treated mice was significantly shorter than control mice ($n = 5$ oxamate, $n = 8$ control; $p < 0.05$, Kaplan–Meier survival comparison followed by Mantel–Cox long-rank test). (C) Spectrograms illustrating the power of EEGs recorded from the cortex from a representative saline- (top) and oxamate-treated (bottom) mouse. Arrows illustrate SE termination. (D) Oxamate reduces high-frequency discharges. A representative EEG trace from saline-injected (top) and oxamate-treated (bottom) mice of 60 min of the self-sustaining SE. Dots represent high-frequency events detected during SE. Note numerous high-frequency discharges in control mice and fewer in oxamate-treated mice. (E) Oxamate reduces the number of high-frequency discharges. Oxamate-treated mice had fewer high-frequency discharges as opposed to saline control mice ($n = 5$ in each group, $p < 0.005$, Kolmogorov–Smirnov test). (F) The median behavioral seizure score (BSS) along with 95% CI in the saline- and oxamate-treated mice. The dotted line indicates the saline/oxamate injection. The self-sustaining phase of SE was scored every 2 min on a Racine scale. Saline-treated mice received significantly higher scores when compared to oxamate-treated mice ($n = 5$ each; $p < 0.005$, two-tailed Mann–Whitney test), which indicates that SE in saline-injected mice was more severe. (G) Termination of SE by oxamate is neuroprotective. Representative images of the hippocampus from saline- and oxamate-treated mice 3 days following SE. Note the widespread neuronal loss in CA1 neurons indicated by the lack of NeuN immunoreactivity in the pyramidal cell layer in saline-treated mice. Green—NeuN, Blue—DAPI. (H) Oxamate protects from neuronal loss in CA1. Quantification of NeuN+ cells in CA1 area ($n = 3$ each; $p < 0.001$; unpaired t -test). (I) Oxamate inhibits lactate production in the brain. Lactate concentration in the brain during SE was measured 15 min before and 15 min after oxamate injection. Oxamate rapidly blocks the production of lactate ($n = 3$; $p < 0.005$; paired t -test, vs. untreated animals, $n = 4$; $p > 0.05$; paired t -test). * p value < 0.05 ; ** p value < 0.005 ; *** p value < 0.001 .

interictal spikes are associated with an increased local cerebral glucose utilization,³⁷ which indicates that glucose metabolism supports, at least to some extent, the generation of postictal epileptiform discharges. Interestingly, postictal spikes were less common in oxamate-treated mice when compared to control mice.

SE is associated with high mortality in experimental animals³⁰ and humans.³⁸ We previously reported that in this model, 33% of mice die during the self-sustaining SE,

with a majority of death occurring in the first hour.³⁰ All mice treated with oxamate survived SE, whereas 25% of control mice died ($n = 5$ oxamate, $n = 8$ control; $p > 0.05$; Fisher test).

We studied neuronal loss following either oxamate or saline treatment to study the effect of oxamate treatment on SE-induced cell death because energy deprivation could exacerbate neuronal death. There is extensive neuronal death in CA1 and CA3 neurons and sporadic cell death in

the dentate hilus following CHS-induced SE.³⁰ Similarly, in saline-injected mice, we found widespread neuronal loss in CA1 neurons, indicated by the lack of NeuN immunoreactivity in the pyramidal cell layer. In oxamate-treated mice, the CA1 pyramidal neurons were intact (Fig. 2G,H) ($n = 3$ each; $p < 0.001$; unpaired t -test), suggesting that oxamate treatment is neuroprotective.

We expected extracellular lactate concentration in the brain to decline following oxamate treatment because it blocks pyruvate-to-lactate conversion. Lactate concentration in the brain during SE 15 min after oxamate injection was less than that 15 min before the injection ($n = 3$; $p < 0.005$; paired t -test). We did not detect similar changes in extracellular lactate concentration in untreated animals ($n = 4$; $p > 0.05$; paired t -test) (Fig. 2I).

Oxamate reduces CA1 network excitability

To further understand the effect of glycolysis inhibition on neuronal excitability, we tested the effect of oxamate on an excited neuronal network with seizure-like events in vitro. Previous studies show excessive and abnormal neuronal activation in hippocampal-parahippocampal circuitry during experimental seizures and SE,^{33,39} and neuronal loss in CA1 following SE.³⁰ We used genetically encoded calcium indicator 7 (GCaMP7) to study neuronal excitability in vitro. We delivered a mix of GCaMP7 and CaMKII-Cre transgenes to the dorsal and ventral CA1 hippocampus to target CA1 excitatory neurons. We prepared acute hippocampal slices 10–14 days after the injection and studied them under a wide-field microscope.

Even modest increases in potassium concentration in the recording solution excite neurons in vitro and can produce epileptiform discharges.⁴⁰ Therefore, we increased potassium concentration in the recording solution from 2 to 5 mM to induce synchronous and asynchronous phasic firing of GCaMP7-expressing neurons.^{40,41} We observed more GCaMP7-expressing neurons with increased tonic green fluorescence and phasic activity (Fig. 3A,B). We then tested the effect of oxamate on the excited neuronal network. We perfused GCaMP7-expressing hippocampal slices with a recording solution containing 3 mM oxamate, which caused a rapid decrease in phasic and tonic GCaMP7 signal. The oxamate wash-out restored a dynamic neuronal response characterized by a rapid increase in tonic GCaMP7 signal and phasic activity (Fig. 3A,B).

We analyzed time-lapse movies of the CA1 cell body layer using ImageJ. Oxamate decreased GCaMP7 fluorescence across the entire CA1 population ($\Delta F/F$ 5 mM vs. $\Delta F/F$ 5 mM K^+ + 3 mM oxamate: 14.54%, 0.64 (mean diff., SE of diff.), $p < 0.0001$, one-way ANOVA, Tukey correction). Tonic GCaMP7 fluorescence increased upon

removing oxamate ($\Delta F/F$ wash-out 5 mM vs. $\Delta F/F$ 5 mM K^+ + 3 mM oxamate: 15.73%, 0.78 (mean diff., SE of diff.), $p < 0.0001$, one-way ANOVA, Tukey correction). Moreover, the post-treatment fluorescence was even brighter than the baseline fluorescence ($\Delta F/F$ wash-out 5 mM vs. $\Delta F/F$ 5 mM K^+ 1.2%, 0.12 (mean diff., SE of diff.), $p < 0.0001$, one-way ANOVA, Tukey correction, $n = 5$ animals, 7 slices) (Fig. 3A,B). These findings suggest that oxamate reduced neuronal excitability. Moreover, a robust neuronal response to the wash-out step indicates that 3 mM oxamate on the brain slices was not toxic.

We also analyzed the response of a single neuron to 3 mM oxamate treatment. We randomly selected five time-lapse movies in selected GCaMP7-tagged neurons. Oxamate reduced the frequency of calcium spikes (Fig. 3C) ($n = 20$ neurons; $p < 0.0001$, Kolmogorov–Smirnov test) and then increased during the wash-out phase (Fig. 3C) ($n = 20$ neurons; $p < 0.005$, Kolmogorov–Smirnov test) (Fig. 3C).

Overall, these findings indicate that oxamate reduces phasic and tonic neuronal activity.

Oxamate reduces excitatory transmission in CA1

We recorded sEPSC from CA1 principal neurons to understand the oxamate effect on excitatory transmission. We found that the application of oxamate significantly reduced the sEPSC frequency, which is evident by the rightward shift in the inter-event interval cumulative fraction probability distribution ($n = 8$ cells; $p < 0.0001$, Kolmogorov–Smirnov test). Interestingly, we did not detect changes in sEPSC amplitude ($n = 8$ cells; $p > 0.05$, Kolmogorov–Smirnov test) (Fig. 4A,B). These findings indicate that oxamate's action may involve presynaptic mechanisms at the excitatory synapse.

Discussion

In summary, we report that (1) a single, non-convulsive seizure and SE strongly stimulate extracellular lactate production and glucose decline; (2) oxamate, a lactate dehydrogenase inhibitor, effectively terminates experimental SE and reduces associated neuronal damage; (3) and oxamate reduces neuronal excitability and inhibits glutamatergic neurotransmission. Our findings highlight that sustaining seizure activity accelerates lactate production, providing in vivo and in vitro evidence that inhibiting lactate dehydrogenase with oxamate effectively reduces neuronal excitability.

Repeated action potentials and enhanced synaptic transmission during seizures produce high metabolic demands, which causes an increase in cerebral blood

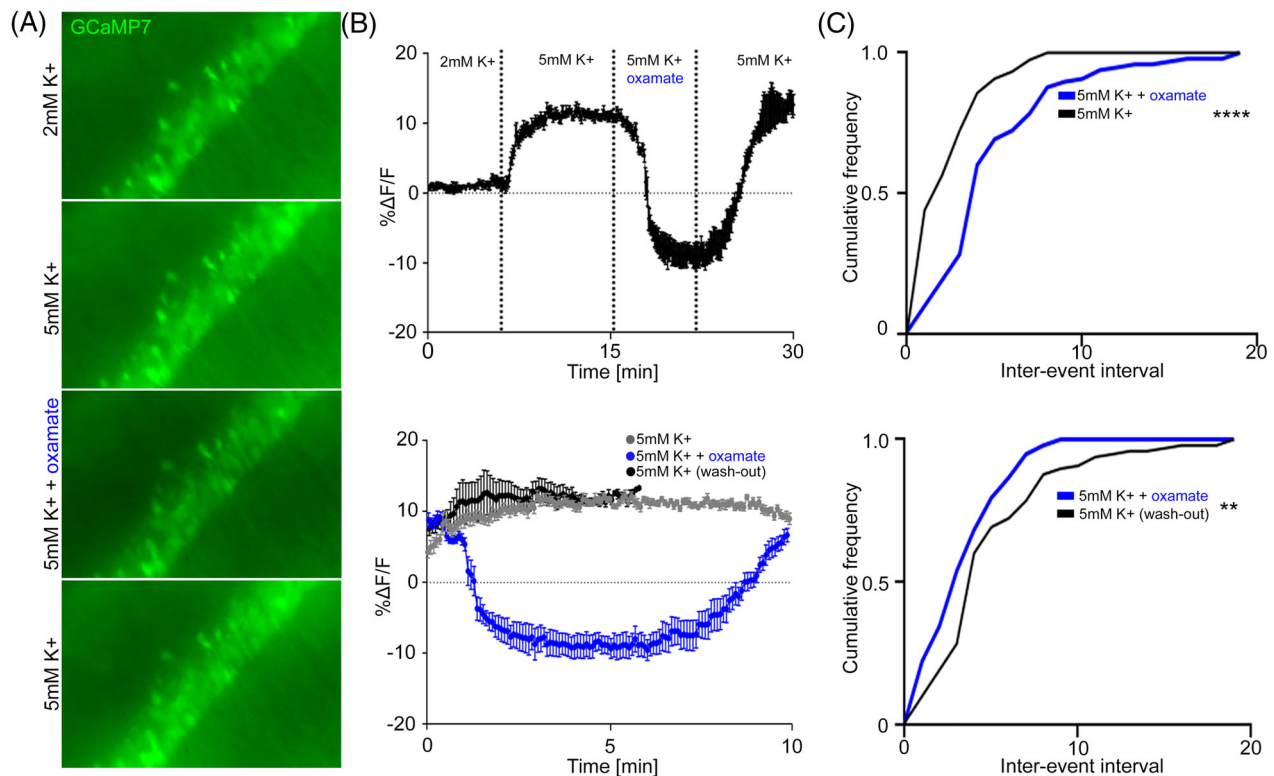


Figure 3. Oxamate reduces neuronal tonic and phasic activity. (A) Representative images from CA1 hippocampus following perfusion with recording solution containing basal (2 mM) K⁺, elevated (5 mM) K⁺, 3 mM oxamate (5 mM K⁺ + oxamate), and wash-out (5 mM K⁺). Note decreased GCaMP7 fluorescence when oxamate was present in the recording solution. (B) Oxamate reduces GCaMP7 fluorescence. Top: Elevated potassium concentration (5 mM) increases GCaMP7 fluorescence in CA1 neuronal population. Perfusion with oxamate decreased GCaMP7 fluorescence and then increased after oxamate wash-out. Bottom: elevated (5 mM), 3 mM oxamate (5 mM K⁺ + oxamate), and wash-out (5 mM K⁺) conditions plotted against the same time frame. Oxamate reduces neuronal tonic network excitability ($\Delta F/F$ 5 mM vs. $\Delta F/F$ 5 mM K⁺ + 3 mM oxamate: 14.54%, 0.64 (mean diff., SE of diff.), $p < 0.0001$, one-way ANOVA, Tukey correction), which reverses when oxamate is washed out from the perfusion system ($\Delta F/F$ wash-out 5 mM vs. $\Delta F/F$ 5 mM K⁺ + 3 mM oxamate: 15.73%, 0.78 (mean diff., SE of diff.), $p < 0.0001$, one-way ANOVA, Tukey correction, $n = 5$ animals, 7 slices). (C) Oxamate reduces phasic firing. Oxamate reduced the frequency of calcium spikes ($n = 20$ neurons; $p < 0.0001$, Kolmogorov–Smirnov test). Calcium spikes became more apparent again when oxamate was washed out from the chamber ($n = 20$ neurons; $p < 0.005$, Kolmogorov–Smirnov test). ** p value < 0.005 ; **** p value < 0.0001 .

flow⁴² to deliver glucose and oxygen. Glycolysis can end with the production of acetyl Co-A from pyruvate, which fuels oxidative phosphorylation; alternately, pyruvate converts to lactate to allow more rapid but less efficient ATP generation. SE represents an extreme form of seizure activity lasting hours to days. Such an abnormally active state would require constant energy replenishment. While oxidative phosphorylation provides more ATP molecules per glucose molecule than glycolysis, 2 ATP molecules generated by the early steps in the glycolytic pathway provide a readily available pool of ATP for firing neurons during SE.⁴³

Several studies have reported serial cerebral microdialysis measures of lactate and glucose in the extracellular fluid in the experimental animals^{44–46} and people with epilepsy.^{47–49} Increased lactate/pyruvate ratio and

decreased extracellular glucose levels are used as a biomarker of a seizure episode and indicate a metabolic crisis associated with a postictal state. We propose that glycolysis-derived energy preferentially fuels seizures and that targeting this metabolic pathway might resolve seizures. The microdialysis method suffers from relatively poor temporal resolution with sampling times of several minutes, which is too slow compared to ictal discharges. Conversely, biosensors continuously monitor extracellular metabolites in the brain with a higher temporal resolution. By combining EEG recordings with biosensor probes, we recorded real-time changes in glucose and lactate levels in the brain in the extracellular space in vivo during a single, non-convulsive seizure and SE. We found that electrographic seizures and SE strongly stimulate glycolysis as lactate concentration increases and glucose

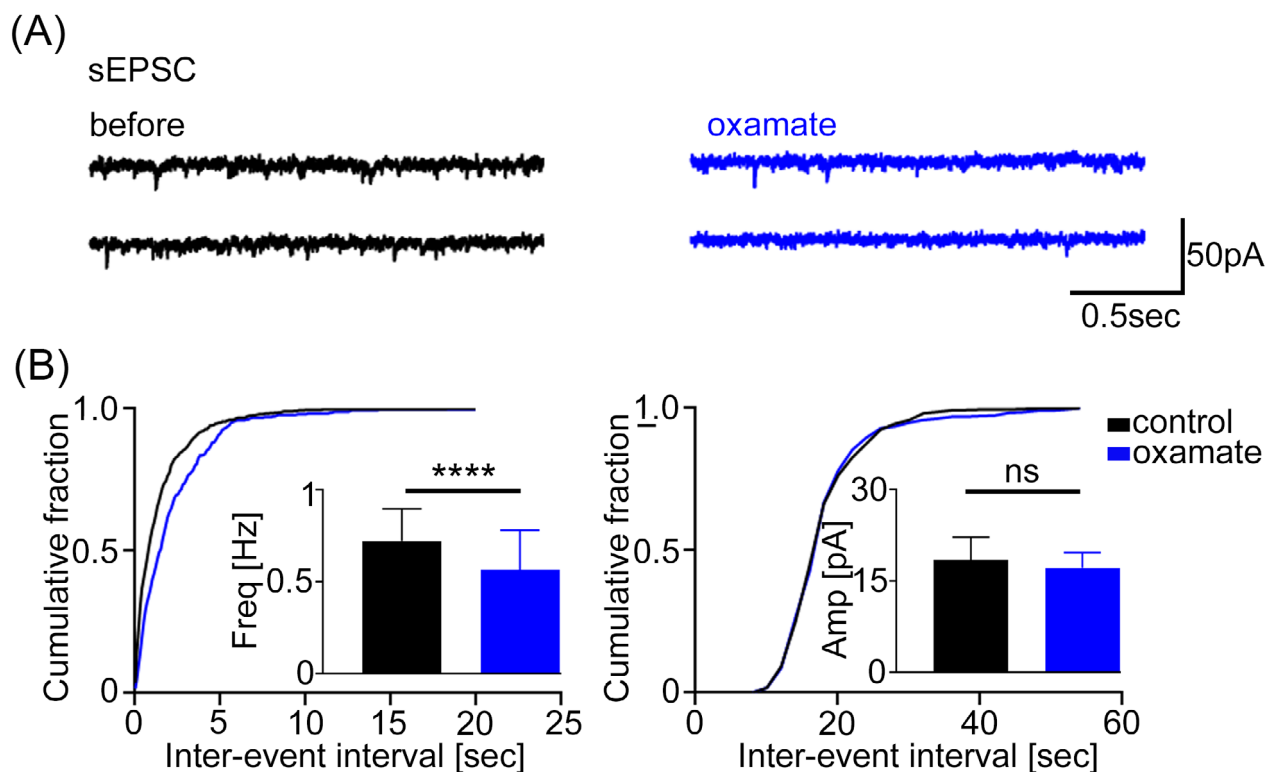


Figure 4. Oxamate reduces the spontaneous excitatory postsynaptic current frequency. (A) Spontaneous excitatory postsynaptic current (sEPSC) was recorded from CA1 neurons before (left) and after (right) application of oxamate. (B) Oxamate reduced sEPSC frequency ($n = 8$ cells, $p < 0.0001$, Kolmogorov–Smirnov test) but not amplitude ($n = 8$ cells, $p > 0.05$, Kolmogorov–Smirnov test) in CA1 principal neurons. **** p value < 0.0001 .

concentration declines in the extracellular space. We also report that high-frequency discharges are associated with increased glucose metabolism and lactate buildup in the extracellular space. The high-frequency discharges are more frequent in the first quartile of SE,³⁰ which coincide with higher anaerobic glycolytic rate, that is, glucose uptake from the extracellular space and lactate release from the cells (Fig. 1).

Astrocytes can provide energy substrates for supporting neurons in an activity-dependent manner. According to Astrocyte to Neuron Lactate Shuttle (ANLS) hypothesis, glutamate uptake into astrocytes stimulates glycolysis and lactate production for the energy needs of neurons.⁵⁰ Thus, seizure-induced glutamate release from neurons may stimulate glycolysis in astrocytes, which can explain lactate accumulation in the extracellular space.

High dependency on glycolysis-derived energy to sustain seizure activity during SE suggests that targeting this metabolic pathway might modulate severe SE. In this study, oxamate, an indirect glycolysis inhibitor, terminated SE, demonstrating the importance of LDH in maintaining SE. Oxamate blocks LDH activity, which catalyzes the interconversion of pyruvate and lactate. During

seizures, extracellular lactate concentration increases (Fig. 1), indicating increased LDH activity.^{23,27} After oxamate treatment, we detected fewer high-frequency discharges and an overall decrease in extracellular lactate concentration. Lack of energy would stop the development of the ATP-demanding, fast discharges in the early stage of SE (Fig. 2).

Finally, inhibition of LDH with oxamate could potentiate neuronal death, as glycolysis-derived ATP is critical for proper neuronal survival. Additionally, the large body of literature suggests lactate acts as a neuroprotective agent in the brain.^{28,51–53} Interestingly, we detected extensive neuronal cell loss in control but not in oxamate-treated mice. Neuronal death following SE is a function of the duration and severity of SE.⁵⁴ Thus, the neuroprotective effect observed in oxamate-treated mice is likely due to the shorter and less severe SE in this group compared to control mice.

For glycolysis to continue, NAD⁺ must be regenerated from NADH, as NAD⁺ is an obligatory substrate for glyceraldehyde-3-phosphate dehydrogenase enzyme. LDH-catalyzed conversion of pyruvate to lactate is one (but not exclusive) source of NAD⁺. Therefore, reduced

LDH-mediated NAD^+ regeneration may slow the glycolytic conversion of glucose to pyruvate. It is unlikely, however, that the oxamate action profoundly blocks the generation of pyruvate. Moreover, as LDH inhibition blocks pyruvate conversion to lactate, this may favor the conversion of pyruvate to acetyl-CoA and its direction to the TCA cycle. Oxamate treatment represents a less invasive metabolic intervention to terminate seizures because it denies actively firing neurons of a readily available ATP source while facilitating glucose oxidation and TCA cycle-mediated energy production. Thus, ATP production may be slower but not abolished.

Our studies link neuronal excitability to brain energetics by showing that LDH inhibition reduces neuronal excitability in vitro, at least in part by altering synaptic transmission. Neurotransmission is metabolically expensive⁵⁵ because it requires ATP to maintain energy-costly steps: maintaining the electrochemical gradient, filling,⁵⁶ and recycling⁵⁷ the synaptic vesicles. Glutamatergic synapses outnumber GABAergic synapses by 9 to 1 in the cerebral cortex.⁵⁸ The v-type proton pump ATPase and vesicular glutamate transporter (VGLUT)⁵⁹ mediate glutamate loading into synaptic vesicles. Thus, ATP availability is a rate-limiting step in glutamate packaging. Glutamate is then released from the presynaptic bouton into the synaptic cleft via exocytosis. Empty vesicles undergo endocytosis in an ATP-dependent fashion. Our studies indicate that oxamate reduces sEPSC frequency and does not affect sEPSC amplitude in CA1 principal neurons. These preliminary observations regarding synaptic transmission require further confirmation and detailed analysis but suggest decreased glutamate release. Thus, oxamate may inhibit energy-dependent glutamate release machinery in the presynaptic terminal.

Finally, intervention with oxamate may induce a shift in cellular pH, and thereby alter neuronal excitability and seizure activity. Although we did not measure pH in vivo, in the in vitro studies, oxamate was applied to hippocampal slices by perfusing them with a buffered aCSF, with a pH of 7.4. Solution exchange in the perfusion system is rapid, and any pH change in extracellular space is unlikely. Notably, acidic pH decreases the excitability of the hippocampal CA1 region. Seizures and SE caused a lactic acid buildup in the extracellular space (Fig. 1), likely acidifying extracellular pH. Acidic pH inhibits NMDA receptors in the hippocampal CA1 neurons.⁶⁰ Acidic pH activates the acid-sensing ion channels (ASICs), preferentially expressed on inhibitory interneurons, increasing their firing and thus reducing CA1 pyramidal neuron excitability.⁶¹ It also causes adenosine release, reducing excitability.⁶² We demonstrate that in vivo intervention with oxamate decreases lactate production in the extracellular space in the brain (Fig. 2), which will have the opposite effect of increasing excitability.

This study has several limitations. We did not simultaneously measure the extracellular glucose and lactate concentration during a single seizure and SE from the same animal. We could not perform dual metabolite measurements because of the large biosensor probe size. We did not place a probe near hippocampal stimulation because it could contaminate or alter the biosensor signal. Additionally, we used a single, high dose of oxamate to investigate its anti-seizure effect. Future studies will examine the impact of oxamate dose on seizure suppression and the chronic effect of oxamate treatment on behavioral and cognitive outcomes and epileptogenesis. We used oxamate to demonstrate that lactate production sustains SE. The potential application of oxamate as an anticonvulsant was proposed earlier.²⁴

Overall, our findings provide an extensive description of the role of lactate-generating glycolysis during a single seizure and SE and an in vivo evidence that blocking lactate production effectively terminates SE.

Author Contributions

Conception and design of the study (DS, JK), acquisition and analysis of data (DS, HS, IK, SS, JW), and writing the manuscript (DS, JK).

Acknowledgements

We want to thank other members of the Kapur laboratory for their valuable comments on this study. This work was supported by the National Institutes of Health (R37 NS119012, R01NS120945, RO1 NS040337) and the UVA Brain Institute.

Conflict of Interest

None of the authors has any conflict of interest to disclose.

References

1. Cervenka MC, Hocker S, Koenig M, et al. Phase I/II multicenter ketogenic diet study for adult superrefractory status epilepticus. *Neurology*. 2017;88(10):938-943.
2. Husari KS, Cervenka MC. The ketogenic diet all grown up—ketogenic diet therapies for adults. *Epilepsy Res*. 2020;162:106319.
3. Martin K, Jackson CF, Levy RG, Cooper PN. Ketogenic diet and other dietary treatments for epilepsy. *Cochrane Database Syst Rev*. 2016;2:CD001903.
4. Kossoff EH, McGrogan JR, Bluml RM, et al. A modified Atkins diet is effective for the treatment of intractable pediatric epilepsy. *Epilepsia*. 2006;47(2):421-424.

5. Thakur KT, Probasco JC, Hocker SE, et al. Ketogenic diet for adults in super-refractory status epilepticus. *Neurology*. 2014;82(8):665-670.
6. Cervenka MC, Hartman AL, Venkatesan A, Geocadin RG, Kossoff EH. The ketogenic diet for medically and surgically refractory status epilepticus in the neurocritical care unit. *Neurocrit Care*. 2011;15(3):519-524.
7. Masino SA, Rho JM. Mechanisms of ketogenic diet action. *Jasper's Basic Mechanisms of the Epilepsies*. National Center for Biotechnology Information (US); 2012.
8. Rogawski MA, Löscher W, Rho JM. Mechanisms of action of antiseizure drugs and the ketogenic diet. *Cold Spring Harb Perspect Med*. 2016;6(5):a022780.
9. Lothman EW, Hatlelid JM, Zorumski CF. Functional mapping of limbic seizures originating in the hippocampus: a combined 2-deoxyglucose and electrophysiologic study. *Brain Res*. 1985;360(1):92-100.
10. Rho JM, Shao L-R, Stafstrom CE. 2-Deoxyglucose and Beta-hydroxybutyrate: metabolic agents for seizure control. *Front Cell Neurosci*. 2019;13:172.
11. Garriga-Canut M, Schoenike B, Qazi R, et al. 2-deoxy-D-glucose reduces epilepsy progression by NRSF-CtBP-dependent metabolic regulation of chromatin structure. *Nat Neurosci*. 2006;9(11):1382-1387.
12. Phelps ME, Huang SC, Hoffman EJ, Selin C, Sokoloff L, Kuhl DE. Tomographic measurement of local cerebral glucose metabolic rate in humans with (F-18)2-fluoro-2-deoxy-D-glucose: validation of method. *Ann Neurol*. 1979;6(5):371-388.
13. Sokoloff L, Reivich M, Kennedy C, et al. The [¹⁴C] deoxyglucose method for the measurement of local cerebral glucose utilization: theory, procedure, and Normal values in the conscious and anesthetized albino Rat1. *J Neurochem*. 1977;28(5):897-916.
14. Shao L-R, Stafstrom CE. Glycolytic inhibition by 2-deoxy-d-glucose abolishes both neuronal and network bursts in an in vitro seizure model. *J Neurophysiol*. 2017;118(1):103-113.
15. Stafstrom CE, Ockuly JC, Murphree L, Valley MT, Roopra A, Sutula TP. Anticonvulsant and antiepileptic actions of 2-deoxy-D-glucose in epilepsy models. *Ann Neurol*. 2009;65(4):435-447.
16. Janicot R, Stafstrom CE, Shao L-R. 2-Deoxyglucose terminates pilocarpine-induced status epilepticus in neonatal rats. *Epilepsia*. 2020;61(7):1528-1537.
17. Abdel-Wahab AF, Mahmoud W, Al-Harizy RM. Targeting glucose metabolism to suppress cancer progression: prospective of anti-glycolytic cancer therapy. *Pharmacol Res*. 2019;150:104511.
18. Vijayaraghavan R, Kumar D, Dube SN, et al. Acute toxicity and cardio-respiratory effects of 2-deoxy-D-glucose: a promising radio sensitizer. *Biomed Environ Sci*. 2006;19(2):96-103.
19. Terse PS, Joshi PS, Bordelon NR, et al. 2-deoxy-d-glucose (2-DG)—induced cardiac toxicity in rat: NT-proBNP and BNP as potential early cardiac safety biomarkers. *Int J Toxicol*. 2016;35(3):284-293.
20. Granchi C, Bertini S, Macchia M, Minutolo F. Inhibitors of lactate dehydrogenase isoforms and their therapeutic potentials. *Curr Med Chem*. 2010;17(7):672-697.
21. Peek CB, Levine DC, Cedernaes J, et al. Circadian clock interaction with HIF1 α mediates oxygenic metabolism and anaerobic glycolysis in skeletal muscle. *Cell Metab*. 2017;25(1):86-92.
22. Augoff K, Hryniewicz-Jankowska A, Tabola R. Lactate dehydrogenase 5: an old friend and a new hope in the war on cancer. *Cancer Lett*. 2015;358(1):1-7.
23. Sada N, Suto S, Suzuki M, Usui S, Inoue T. Upregulation of lactate dehydrogenase a in a chronic model of temporal lobe epilepsy. *Epilepsia*. 2020;61(5):e37-e42.
24. Sada N, Lee S, Katsu T, Otsuki T, Inoue T. Targeting LDH enzymes with a stiripentol analog to treat epilepsy. *Science*. 2015;347(6228):1362-1367.
25. Rho JM, Boison D. The metabolic basis of epilepsy. *Nat Rev Neurol*. 2022;18(6):333-347.
26. Rho JM. Inhibition of lactate dehydrogenase to treat epilepsy. *N Engl J Med*. 2015;373(2):187-189.
27. Ksendzovsky A, Bachani M, Altshuler M, et al. Chronic neuronal activation leads to elevated lactate dehydrogenase a through the AMP-activated protein kinase/hypoxia-inducible factor-1 α hypoxia pathway. *Brain Commun*. 2023;5(1):fcac298.
28. Skwarzynska D, Sun H, Williamson J, Kasprzak I, Kapur J. Glycolysis regulates neuronal excitability via lactate receptor, HCA1R. *Brain*. 2023;146(5):1888-1902.
29. Racine RJ. Modification of seizure activity by electrical stimulation. II. Motor seizure. *Electroencephalogr Clin Neurophysiol*. 1972;32(3):281-294.
30. Lewczuk E, Joshi S, Williamson J, Penmetza M, Shan S, Kapur J. Electroencephalography and behavior patterns during experimental status epilepticus. *Epilepsia*. 2018;59(2):369-380.
31. Adotevi N, Lewczuk E, Sun H, et al. α -Amino-3-hydroxy-5-methyl-4-isoxazolepropionic acid receptor plasticity sustains severe, Fatal Status Epilepticus. *Ann Neurol*. 2020;87(1):84-96.
32. Mazurkiewicz M, Kambham A, Pace B, Skwarzynska D, Wagley P, Burnsed J. Neuronal activity mapping during exploration of a novel environment. *Brain Res*. 2022;1776:147748.
33. Burnsed J, Skwarzynska D, Wagley PK, Isbell L, Kapur J. Neuronal circuit activity during neonatal hypoxic-ischemic seizures in mice. *Ann Neurol*. 2019;86(6):927-938.
34. Singh T, Batabyal T, Kapur J. Neuronal circuits sustaining neocortical-injury-induced status epilepticus. *Neurobiol Dis*. 2022;165:105633.

35. Sun J, Kapur J. M-type potassium channels modulate Schaffer collateral-CA1 glutamatergic synaptic transmission. *J Physiol.* 2012;590(16):3953-3964.
36. Pottkämper JCM, Hofmeijer J, van Waarde JA, van Putten MJAM. The postictal state — what do we know? *Epilepsia.* 2020;61(6):1045-1061.
37. Chugani HT, Shewmon DA, Khanna S, Phelps ME. Interictal and postictal focal hypermetabolism on positron emission tomography. *Pediatr Neurol.* 1993;9(1):10-15.
38. DeLorenzo RJ, Hauser WA, Towne AR, et al. A prospective, population-based epidemiologic study of status epilepticus in Richmond, Virginia. *Neurology.* 1996;46(4):1029-1035.
39. Dabrowska N, Joshi S, Williamson J, et al. Parallel pathways of seizure generalization. *Brain.* 2019;142(8):2336-2351.
40. Hablitz JJ, Lundervold A. Hippocampal excitability and changes in extracellular potassium. *Exp Neurol.* 1981;71(2):410-420.
41. Stringer JL, Lothman EW. Epileptiform discharges induced by altering extracellular potassium and calcium in the rat hippocampal slice. *Exp Neurol.* 1988;101(1):147-157.
42. Holtzman D, Mulkern R, Meyers R, et al. In vivo phosphocreatine and ATP in piglet cerebral gray and white matter during seizures. *Brain Res.* 1998;783(1):19-27.
43. Pfeiffer T, Schuster S, Bonhoeffer S. Cooperation and competition in the evolution of ATP-producing pathways. *Science.* 2001;292(5516):504-507.
44. Imran I, Hillert MH, Klein J. Early metabolic responses to lithium/pilocarpine-induced status epilepticus in rat brain. *J Neurochem.* 2015;135(5):1007-1018.
45. Thoresen M, Hallström Å, Whitelaw A, et al. Lactate and pyruvate changes in the cerebral gray and white matter during Posthypoxic seizures in newborn pigs. *Pediatr Res.* 1998;44(5):746-754.
46. Darbin O, Risso JJ, Carre E, Lonjon M, Naritoku DK. Metabolic changes in rat striatum following convulsive seizures. *Brain Res.* 2005;1050(1):124-129.
47. Vespa P, Tubi M, Claassen J, et al. Metabolic crisis occurs with seizures and periodic discharges after brain trauma. *Ann Neurol.* 2016;79(4):579-590.
48. During MJ, Fried I, Leone P, Katz A, Spencer DD. Direct measurement of extracellular lactate in the human hippocampus During spontaneous seizures. *J Neurochem.* 1994;62(6):2356-2361.
49. Cornford EM, Shamsa K, Zeitzer JM, et al. Regional analyses of CNS microdialysate glucose and lactate in seizure patients. *Epilepsia.* 2002;43(11):1360-1371.
50. Magistretti PJ, Sorg O, Naichen Y, Pellerin L, de Rham S, Martin JL. Regulation of astrocyte energy metabolism by neurotransmitters. *Ren Physiol Biochem.* 1994;17(3-4):168-171.
51. Roumes H, Dumont U, Sanchez S, et al. Neuroprotective role of lactate in rat neonatal hypoxia-ischemia. *J Cereb Blood Flow Metab.* 2021;41(2):342-358.
52. Schurr A. Lactate: a major and crucial player in normal function of both muscle and brain. *J Physiol.* 2008;586(Pt 11):2665-2666.
53. Berthet C, Lei H, Thevenet J, Gruetter R, Magistretti PJ, Hirt L. Neuroprotective role of lactate after cerebral ischemia. *J Cereb Blood Flow Metab.* 2009;29(11):1780-1789.
54. Fujikawa DG. The temporal evolution of neuronal damage from pilocarpine-induced status epilepticus. *Brain Res.* 1996;725(1):11-22.
55. Harris JJ, Jolivet R, Attwell D. Synaptic energy use and supply. *Neuron.* 2012;75(5):762-777.
56. Ueda T, Naito S. Specific inhibition of the phosphorylation of protein I, a synaptic protein, by affinity-purified anti-protein I antibody. *Prog Brain Res.* 1982;56:87-103.
57. Ashrafi G, Wu Z, Farrell RJ, Ryan TA. GLUT4 mobilization supports energetic demands of active synapses. *Neuron.* 2017;93(3):606-615.e3.
58. Attwell D, Laughlin SB. An energy budget for signaling in the grey matter of the brain. *J Cereb Blood Flow Metab.* 2001;21(10):1133-1145.
59. Carlson MD, Ueda T. Accumulated glutamate levels in the synaptic vesicle are not maintained in the absence of active transport. *Neurosci Lett.* 1990;110(3):325-330.
60. Vyklický L Jr, Vlachová V, Krůsek J. The effect of external pH changes on responses to excitatory amino acids in mouse hippocampal neurones. *J Physiol.* 1990;430(1):497-517.
61. Weng J-Y, Lin Y-C, Lien C-C. Cell type-specific expression of acid-sensing ion channels in hippocampal interneurons. *J Neurosci.* 2010;30(19):6548-6558.
62. Dulla CG, Dobelis P, Pearson T, Frenguelli BG, Staley KJ, Masino SA. Adenosine and ATP link PCO₂ to cortical excitability via pH. *Neuron.* 2005;48(6):1011-1023.